Numerical analysis of the dynamic response of an open landslide slope under seismic loading

Xiangling Li[1], Changyong Liu[2,*]

[1]Shanxi Metallurgical Geotechnical Engineering Investigation Co., Ltd., Taiyuan, 030000, China
[2]The Third Bureau of Metallurgical Geology Administration of China, Taiyuan, 030000, China

670350203@qq.com, *530142042@qq.com

Abstract. Earthquakes are very likely to produce various geological disasters, and it is very important to study the stability and deformation characteristics of slopes under the action of earthquakes. In this paper, a three-dimensional numerical model of slope considering the structural section of rock body is established with an open slide slope as the research object, and the numerical simulation of seismic load is carried out for the slope based on the time-range analysis method. The results show that the steep slope responds to the seismic loading to a greater extent, and its displacement deformation is more obvious than that at the bottom of the rock body. The potential sliding surface formed by the slope is connected with the fault of the rock body, forming a more significant plastic through zone. With the increase of seismic load amplitude, the overall trend of PGA amplification coefficient is more obvious, showing the free surface amplification effect. With the increase of the slope height, the amplification effect has a certain attenuation trend.

Keywords: Structural section; Seismic loading; Dynamic response characteristics; PGA; Numerical simulation.

1 Introduction

In order to match the mining production capacity and to increase economic benefits by maximizing resource recovery, comprehensive measures must be taken to improve mining safety and production capacity. According to statistics and investigations, landslides are the most common geological disasters after earthquakes [1]. Currently, the research on seismic slope response methods mainly includes field seismic analysis, theoretical analysis, experimental research, and numerical simulation. Qi Shengwen et al. [2] studied and analyzed the stability of slopes under seismic action from the principles of engineering geology, suggesting that the main cause of slope instability and failure under seismic action is the coupling effect of seismic inertial force and superstatic pore water pressure. Huang Runqiu et al. [3] collected geological disaster data after the Wenchuan earthquake and analyzed the geological disasters caused by various factors, concluding that the distribution pattern of seismic geological disasters distinctly exhibits

P. Liu et al. (eds.), *Proceedings of the 2024 5th International Conference on Civil, Architecture and Disaster Prevention and Control (CADPC 2024)*, Atlantis Highlights in Engineering 31,
https://doi.org/10.2991/978-94-6463-435-8_23

an overburden effect; landslides are prone to occur in soft rocks, while collapses are more common in hard rocks. In 1950, Terzaghi [4] first used the pseudo-static method to analyze the stability of earthquake slopes, introducing the horizontal seismic force coefficient. Chopra [5] proved that the stability of earthquake slopes is significantly affected by the vertical seismic force. Li Guo et al. [6] calculated the seismic response of slope models with and without weak base using the pseudo-dynamic method and found that the weak base has a certain degree of isolation effect before the slope fails, which is conducive to slope stability. After the overall failure of the slope, the weak base will exacerbate the extension and penetration of the rupture surface, leading to landslides. Teng Guangliang et al. [7] used the discrete element method to establish a two-dimensional discrete element model of rock slopes with two sets of joints, and studied the influence of various factors on the stability of slopes under seismic action, concluding that the instability of jointed rock slopes under seismic action is primarily due to the gradual extension of the tension zone to the shear zone, resulting in combined tension and shear failure. Lu Yulin et al. [8] conducted a study on sandy slope, analyzing the slope using the pseudo-dynamic method under seepage flow conditions, and discussed the impact of seepage flow on the safety factor of the slope. Chakraborty et al. [9] conducted stability analyses of a tailings dam using both the pseudo-static and dynamic methods, clearly indicating the shortcomings of the traditional pseudo-static method. He Liu et al. [10] established a three-dimensional model of an ideal slope and discussed the impact of slope surface morphology on the distribution patterns of acceleration, velocity, and displacement under seismic action through dynamic calculations, concluding that the amplification factor is highest in the concave-convex parts of the slope surface, and the stronger the concavity and convexity, the more significant the amplification.

Based on the above situation, this article focuses on a landslide slope west of a copper mine as the research object, establishing a three-dimensional numerical model of the slope. Leveraging the analytical advantages of Flac3D software, a numerical analysis of the stability of the slope under seismic load is conducted. The results of the numerical simulation will be further studied to understand the dynamic response patterns of the slope under seismic load, providing a theoretical basis for the safe production and engineering protection of slope projects.

2 Overview of project

The mining area is located in hilly and valley terrain. The central area is characterized by hilly terrain formed by the intense weathering of breccia, spreading from east to west, forming a comb-like topography. The highest point is an eastern peak with an elevation of 487.34 meters, while the lowest point in the valley is around 40 meters above sea level, resulting in a relative height difference of 447.34 meters. The northern slope is gentler with a gradient of 20 to 25 degrees, while the southern slope is steeper with a gradient of approximately 35 degrees, creating a pattern of higher elevation to the east and lower elevation to the west in the mining area. A survey was conducted on the structural planes of the open-pit slope west of a copper mine, focusing on the mid-

sections at depths of -254m and -260m. The distribution characteristics of these structural planes were analyzed to study the sliding failure mode of the slope.

The characteristics of the structural planes are as follows: There are two dominant sets of structural planes: one set dips at 55º to 72º, with a steep dip angle (65º to 88º) accounting for the majority at 52.9%, while moderately steep dip angles (34º to 57º) account for 39.2%, and gentle dip angles (10º to 27º) account for 7.9%. There are two dominant sets of structural planes: one set dips at 16º to 71º, with the majority having steep dip angles (61º to 89º), accounting for 70.3%, and moderately steep dip angles (38º to 59º) accounting for 29.7%. According to the geological section division data, the physical and mechanical parameters of the rock mass at the section are shown in Table 1.

Table 1. Physical-mechanical parameters of rock mass on landslide slopes

Type	γ(g/cm^3)	E(MPa)	μ	T(MPa)	C(MPa)	Φ(º)
Breccia	2.94	13500	0.15	0.2	0.16	31.2
Marble	2.74	65000	0.29	2.13	0.6	35

To investigate the impact of seismic conditions on slope stability, standard slope sections were extended to form a three-dimensional finite element model. Initially, the sections were extended into a solid in CAD, followed by the export of the three-dimensional model files. The meshing and material grouping of the three-dimensional model were achieved using ANSYS finite element software, with hexahedral mesh division adopted for the overall model. Subsequently, the generated finite element model was imported into Flac3D for numerical calculations using a plugin. The finite element model comprised 5904 mesh elements, with dimensions of 830m in length, 100m in width, and 460m in height. The slope area was divided based on the rock mass types in the section.

The time-history analysis method is also known as the direct dynamic method or step-by-step integration method. The equation governing the motion of structures under seismic action is:

$$[m]\{\ddot{x}\} + [c]\{\dot{x}\} + [k]\{x\} = -[m]\{1\}\ddot{x_g} \tag{1}$$

The time-history analysis method is based on specific seismic motion and structural models, as well as the constitutive force-deformation relationships of structural elements. It directly integrates the dynamic equation (1) step by step to obtain numerical solutions of structural responses (displacement, velocity, acceleration) as a function of time.

The seismic fortification intensity of the site is rated as 6 degrees, in accordance with the national "Code for Seismic Design of Buildings" (GB50011-2001). Considering various uncertain factors that may have negative effects on the stability of the landslide slope, the seismic fortification intensity of a certain copper mining area is raised by one level in the analysis. Seismic waves that have been recorded nearby are used as the seismic waves for this analysis. The peak ground acceleration of seismic load curve (Figure 1) for earthquakes at this intensity level is 0.15g, and the earthquake wave frequency is 2.0Hz. In order to systematically analyze the changes in the stability of slopes

under different seismic intensities, three seismic intensities are chosen: the design seismic intensity, one level higher than the design seismic intensity, and one level lower than the design seismic intensity. The seismic fortification intensity levels correspond to 6, 7, and 8 degrees, with corresponding seismic wave acceleration amplitudes of 0.05g, 0.15g, and 0.30g, respectively. The amplitude of the earthquake wave is calculated by adjusting the original seismic wave according to Equation (2).

$$a'(t) = \frac{A'max}{A_{max}} a(t) \tag{2}$$

where,$a'(t)$, A'_{max} are the adjusted seismic acceleration time history curve and its peak values,$a(t)$, $A_{max}$are the initial seismic acceleration time history curve and its peak values.

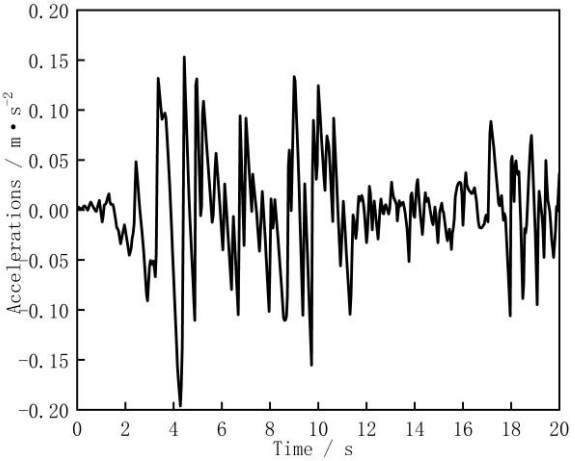

Fig. 1. Seismic wave acceleration time-course curves

3 Numerical Simulation Results and Analysis

3.1 Characteristics of initial ground stress equilibrium

Figures 2(a)-(b) show the contour maps of equivalent stress and average stress distribution of the slope under natural conditions. From the figures, it can be seen that the maximum value of equivalent stress is mainly concentrated at the bottom of the slope, with a maximum value of 14.3 MPa, while the equivalent stress values on the slope surface and in the shallow areas are relatively small, with a minimum value of 0.1 MPa. The distribution pattern of average stress is similar to that of equivalent stress. It is also observed that at a certain elevation, the average stress begins to show negative values, with the negativity increasing as the elevation decreases. Figures 2(c)-(d) depict the contour maps of equivalent strain and shear strain distribution of the slope under natural conditions. The figures indicate that the larger equivalent strain values mainly appear at the positions of rock structure sections, with significantly noticeable plastic strain

values at the steeper sections of the slope top, and the other large plastic strain values mainly concentrated at the foot of the slope. Due to the combined action of tensile and compressive stresses on the slope, shear strain occurs at the positions of rock structure sections, the top, and the foot of the slope, with a maximum shear strain value of 0.013. Influenced by the self-weight and the sliding surface, the maximum shear stress mainly appears at the foot of the slope. Overall, at this stage, the shear strain values of the slope are relatively small, and there are no distinctly visible plastic penetration areas in the soil excavation region; the overall slope is in a stable state.

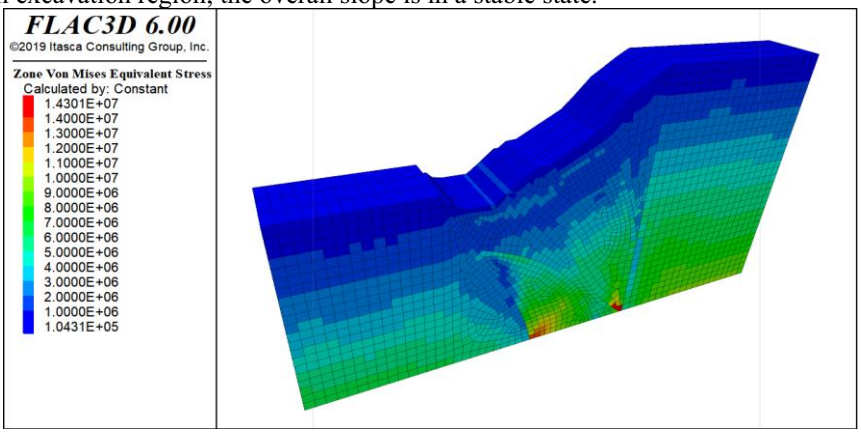

(a)Equivalent stress

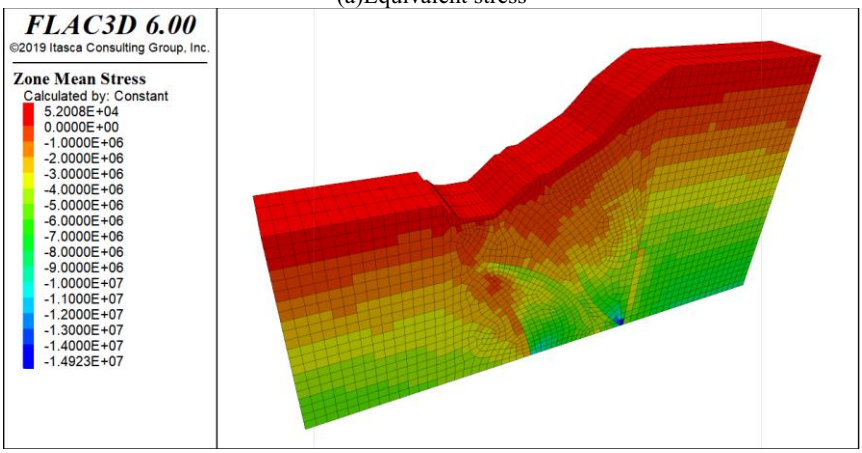

(b)Average stress

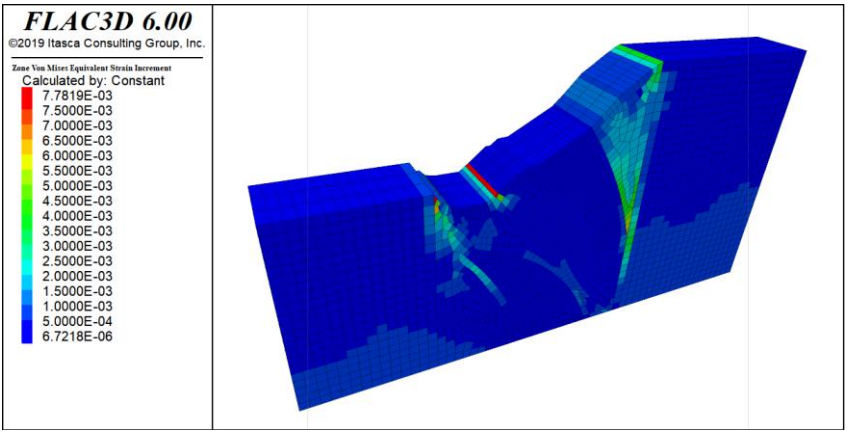

(c)Equivalent strain

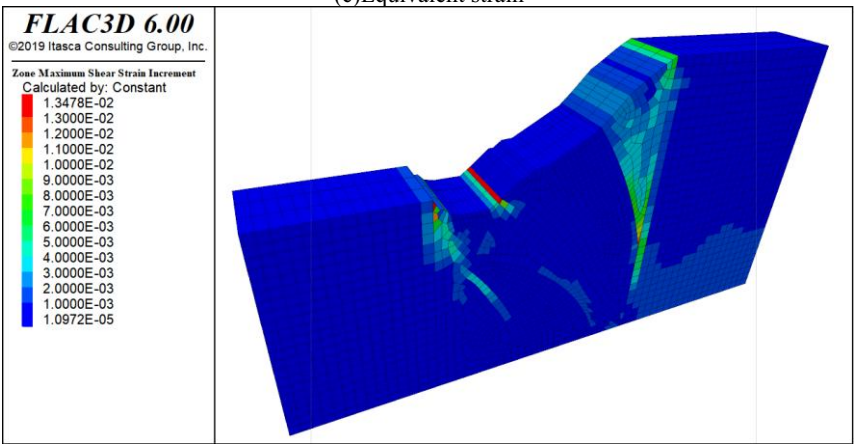

(d)Shear strain

Fig. 2. Characterization of slope cloud maps under natural conditions

3.2 Characteristics of displacement time history curve under seismic load

Figure 3 shows the displacement time history curves at characteristic points on the slope top, middle, and foot. From the figure, it can be observed that the displacement in the x-direction at the characteristic points of the slope top, middle, and foot is significantly increasing, showing an oscillating upward trend with the loading of the seismic waves. The final displacements at the slope top and middle characteristic points are both 0.13m, while the final displacement at the foot characteristic point is the smallest at 0.08m. In terms of the displacement time history curve in the z-direction, the sensitivity of displacement response at the characteristic point at the slope top is higher, with a final displacement of 0.33m, while the sensitivity at the foot and middle characteristic points is lower, with final displacements of 0.06m. The characteristic features of the vector displacement time history curve are similar to those of the z-direction. The final

vector displacement at the slope top is 0.35m, while at the middle and foot, the final vector displacements are 0.13m and 0.09m, respectively.

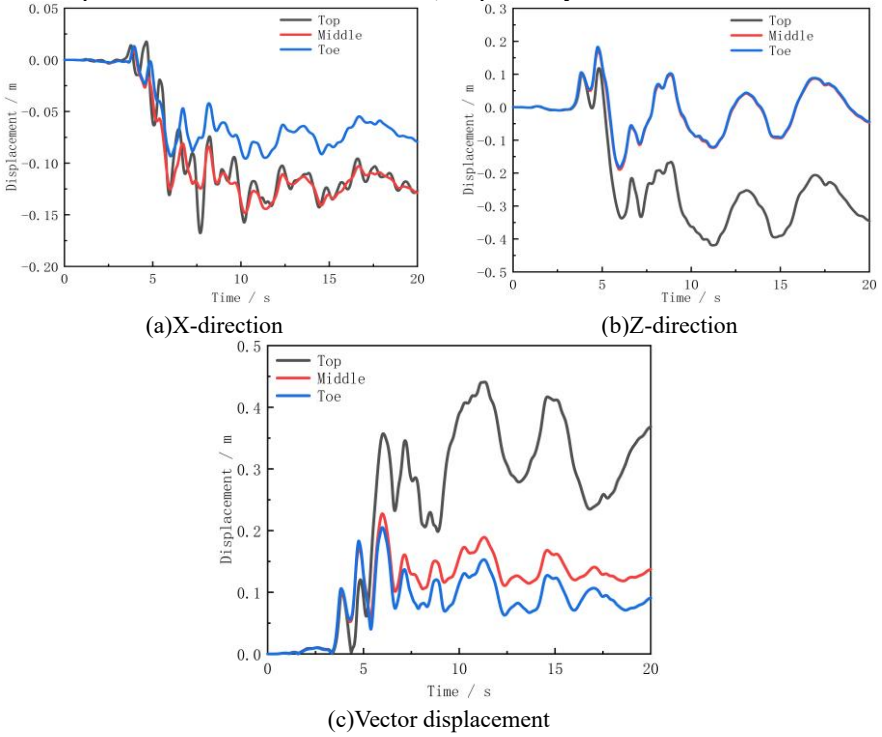

Fig. 3. Displacement time history curves of different monitoring points under seismic loading

3.3 The influence of seismic wave loading amplitude on the PGA characteristics

The PGA (Peak Ground Acceleration) amplification factor of a slope under seismic loading is the basis for slope engineering seismic warning, slope structure reinforcement design, and intensity rapid reporting technology. It can serve as a good indicator of seismic motion intensity. To better study the influence of seismic wave loading amplitude on the dynamic response of the slope, a curve showing the relation between the PGA amplification factor and the horizontal height of monitoring points under different loading amplitudes was plotted, as shown in Figure 4. From Figure 4, it can be observed that the PGA amplification factor shows a trend of initially increasing and then decreasing with the horizontal height of the slope. With the increase in seismic wave loading amplitude, the overall variation trend of the PGA amplification factor becomes more pronounced, demonstrating the amplification effect at the free surface. As the height of the slope increases, there is a certain attenuation in the amplification effect. In the case of rocky slopes subjected to seismic loading, the shear strain and stiffness of the slope body almost remain unchanged. The PGA amplification factor exhibits a clear linear relationship with the increase in seismic wave loading amplitude, indicating that the

proportion of the PGA amplification factor to the seismic wave loading amplitude has a linear characteristic. This phenomenon differs from the conclusions drawn for soil slopes, which indicates that under the same conditions, the seismic wave loading amplitude is not the primary factor affecting the degree of dynamic response amplification in different parts of the slope. It depends more on the composition, structure, physical and mechanical properties of the rock material, as well as the vibration wave frequency spectrum characteristics.

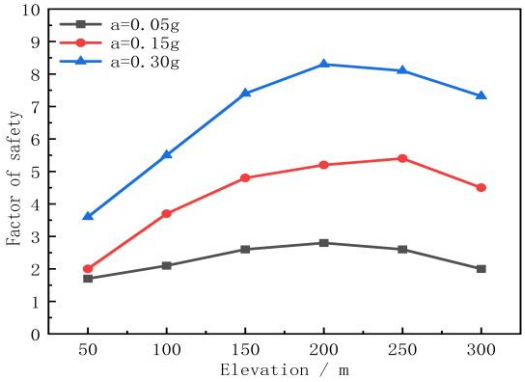

Fig. 4. PGA amplification factor as a function of height

4 Conclusions

1. Under seismic loading, the displacement trend at the slope surface is particularly significant, with steeper slopes exhibiting a greater response to seismic loading, and their displacement and deformation are more pronounced compared to the bottom of the rock mass.
2. A potential sliding surface is formed by the slope, connecting to the rock structure section, creating a significant plastic penetration zone.
3. The PGA amplification factor shows a trend of initially increasing and then decreasing with the horizontal height of the slope. With an increase in seismic wave loading amplitude, the overall trend of the PGA amplification factor becomes more pronounced, indicating a free surface amplification effect.

Reference

1. Zhang, Y., Cheng, Y., Yao, X., et al. (2013). Formation and evolution of the seismic-landslide-debris flow disaster chain in Wenchuan, Sichuan. Geological Bulletin, 32(12), 1900-1910.
2. Qi, S., Wu, F., Liu, C., et al. (2004). Engineering geological analysis of seismic slope stability. Chinese Journal of Rock Mechanics and Engineering, 16, 2792-2797.

3. Huang, R., Li, W. (2008). Study on the development and distribution of geological hazards triggered by the “5.12” Wenchuan earthquake. Chinese Journal of Rock Mechanics and Engineering, 27(12), 2585-2592.
4. Terzaghi, K. (1950). Mechanism of landslides. In S. Paige (Ed.), Application of Geology to Engineering Practice (pp. 83-123). Geological Society of America.
5. Chopra, A. (1967). Earthquake response of earth dams. Journal of the Soil Mechanics and Foundation Engineering Division ASCE, 93(SM2), 65-81.
6. Li, G., Huang, R., Ju, N., et al. (2011). Research on the seismic fracturing mechanism of soft foundation landslides. Journal of Engineering Geology, 19(05), 712-718.
7. Teng, G., Chen, Y., Shi, Y., et al. (2013). Study on influencing factors of the stability of jointed rock slopes under seismic action. Journal of Seismological Engineering, 35(01), 119-125.
8. Lu, Y., Bo, J., Chen, X., et al. (2017). Calculation of seismic stability of sandy slopes considering seepage and earthquake. Journal of Chongqing University, 40(01), 65-75.
9. Chakraborty, D., Choudhury, D. (2013). Pseudo-static and pseudo-dynamic stability analysis of tailings dam under seismic conditions. Proceedings of the National Academy of Sciences India, 83(1), 63-71.
10. He, L., Wu, G., Xie, C., et al. (2013). Dynamic response of three-dimensional solid slopes to seismic waves. Journal of Southwest Jiaotong University, 48(01), 55-61.